PUMA Overexpression Induces Reactive Oxygen Species Generation and Proteasome-Mediated Stathmin Degradation in Colorectal Cancer Cells

Zhihe Liu,[1] Huimei Lu,[1] Honglian Shi,[2] Yuchun Du,[3] Jian Yu,[4] Sheng Gu,[3] Xian Chen,[3] Ke Jian Liu,[2] and Chien-an A. Hu[1]

[1]Department of Biochemistry and Molecular Biology, University of New Mexico School of Medicine and [2]The EPR Center and Toxicology Program, University of New Mexico Health Sciences Center, Albuquerque, New Mexico; [3]Biosciences Division, Los Alamos National Laboratory, Los Alamos, New Mexico; and [4]Department of Pathology, Cancer Institute, University of Pittsburgh, Pittsburgh, Pennsylvania

Abstract

Increased amounts of reactive oxygen species (ROS) induce apoptosis in mammalian cells. PUMA (P53 up-regulated modulator of apoptosis), a mitochondrial proapoptotic BH3-only protein, induces rapid apoptosis through a Bax- and mitochondria-dependent pathway. However, the molecular basis of PUMA-induced apoptosis is largely not understood. Using a combination of biophysical and biochemical methods and PUMA-inducible colorectal cells, DLD-1.PUMA, we showed that (*a*) PUMA-induced apoptosis is dose and time dependent; (*b*) PUMA-induced apoptosis is directly associated with ROS generation; (*c*) diphenyleneiodonium chloride, a ROS blocker, or BAX-inhibiting peptide, a suppressor of BAX translocation, decreased ROS generation and apoptosis in DLD-1.PUMA cells; (*d*) overexpression of *PUMA* induced up-regulation (>1.34-fold) of peroxiredoxin 1 and down-regulation (by 25%) of stathmin through proteasome-mediated degradation; and (*e*) hydrogen peroxide down-regulated stathmin and disrupted the cellular microtubule network. Our findings indicate that PUMA induces apoptosis, in part, through the BAX-dependent generation of superoxide and hydrogen peroxide. ROS overproduction and oxidative stress induce proteome-wise alterations, such as stathmin degradation and disorganization of the cell microtubule network, in apoptotic cells. (Cancer Res 2005; 65(5): 1647-54)

Introduction

Mitochondria-mediated apoptotic programmed cell death involves signaling pathways that induce various protein responses (e.g., posttranslational modification, conformational change, and interorganelle translocation of specific proteins), alteration of mitochondrial membrane permeability, release of apoptogenic factors (e.g., cytochrome *c* and apoptosis-inducing factor), and activate caspases (1–6). P53, a tumor suppressor protein, plays a pivotal role in regulating cell cycle arrest, differentiation, and apoptosis (7, 8). The elevated expression of *p53* leads to mitochondrial-mediated apoptosis, in part through the overproduction of reactive oxygen species (ROS; refs. 9–11). Genes that are directly involved in the generation of ROS are induced in *p53*-mediated apoptotic pathways (8, 9). For example, one of the *p53*-inducible genes, *PIG6* or proline oxidase, when overexpressed in cancer cells, triggers ROS generation and apoptosis (12, 13). Interestingly, ROS themselves are regulators of *p53* and play roles downstream of mitochondria during destruction of the cellular components mediated by activated caspases (7, 14). Interruption of ROS homeostasis is involved in the pathophysiology of cancer. Under normal circumstances, cells respond to oxidative insults by activating various antioxidant defense systems, such as antioxidant enzymes [e.g., superoxide dismutase (SOD), glutathione transferase, glutathione peroxidase, and catalase] and antioxidant proteins (e.g., thioredoxin, peroxiredoxin), to counteract the possible damage induced by oxidants (15, 16). Several members of the Bcl-2 family are involved in ROS-mediated apoptosis (6, 17–20). For example, BAX, a proapoptotic protein and a *p53* downstream target, has been shown to be involved in the induction of a pro-oxidant state and ROS generation in neurons. *BAX* gene dosage determines ROS levels during neuronal apoptosis (21, 22). Another proapoptotic member and a direct *p53* downstream target, PUMA (P53 up-regulated modulator of apoptosis), is inducible by exposure to DNA-damaging agents and by *p53* overexpression and is essential for apoptosis induced by *p53*, hypoxia, and DNA-damaging agents (23–26). We previously showed that PUMA, a mitochondrial BH3-only protein, induces BAX-dependent apoptosis that relies on mitochondrial translocation and multimerization of Bax. Genetic disruption of BAX makes cells resistant to the apoptosis resulting from *PUMA* overexpression in colorectal cancer cells (26). Furthermore, recent studies using *PUMA* knockout mice confirmed that PUMA is required for P53-dependent apoptosis (27, 28).

Activation of *p53* and *p53* downstream targets by chemotherapeutic drugs (e.g., taxanes) alters functions of the microtubule network (29, 30). For example, stathmin, a ubiquitous cytosolic phosphoprotein, is a regulator of the polymerization of microtubules. In its unphosphorylated form, stathmin promotes depolymerization of microtubules and enhances microtubule dynamics by increasing the frequency of catastrophes (31). In addition, stathmin regulates cell cycle progression and its expression is up-regulated in a variety of cancers (e.g., acute leukemia and liver cancer; refs. 32, 33). Finally, two independent studies have shown that overexpression of *p53* decreases stathmin expression through yet undefined mechanisms (34, 35).

Using dihydroethidium staining and electron paramagnetic resonance (EPR) spectrometry, we observed ROS generation in PUMA-overexpressing cells. Overproduction of ROS in apoptotic PUMA-inducible colorectal cancer cells (DLD-1.PUMA) was further

Note: Supplementary data for this article are available at Cancer Research Online (http://cancerres.aacrjournals.org/).

Requests for reprints: Chien-an A. Hu, Department of Biochemistry and Molecular Biology, MSC08 4670 1, University of New Mexico, Albuquerque, NM 87131-001. Phone: 505-272-8816; Fax: 505-272-6587; E-mail: ahu@salud.unm.edu.

confirmed by blocking with diphenyleneiodonium, a ROS inhibitor, and BAX-inhibiting peptide. Employing proteomic methodologies, we showed that overexpression of PUMA increases expression of peroxiredoxin 1 and heat shock protein 70, two oxidative stress–triggered proteins, and decreases stathmin levels through a proteasome-mediated mechanism.

Materials and Methods

Chemicals and Reagents. The deuterium (D)-labeled amino acid [4,4,5,5-D4]lysine (Lys_{D4}) was purchased from Cambridge Isotope (Andover, MA) as previously described (36, 37). Doxycycline, diphenyleneiodonium, dihydroethidium, DMSO, hydrogen peroxide (H_2O_2), formaldehyde, *N*-Acetyl-Leu-Leu-Norleu-al (ALLN), Hoechst 33258 and reagents used for proteomics analysis were purchased from Sigma (St. Louis, MO). Hygromycin B was purchased from EMD Biosciences (La Jolla, CA). α-MEM was purchased from Invitrogen (Carlsbad, CA). McCoy medium, DMEM, regular and dialyzed fetal bovine serum and antimicrobial reagents were obtained from Cellgro (Mediatech, Herndon, PA). Diphenyleneiodonium (2 mmol/L) and dihydroethidium (2 μmol/L) were dissolved in DMSO and kept at −20°C as stock solutions.

Cell Culture, *In vivo* Amino Acid–Coded Tagging of Proteome, and Induction of Apoptosis. PUMA-inducible human colorectal cancer cell lines, DLD-1.PUMA (*p53* null) and the control cell line DLD-1.vector and PUMA antibody were kind gifts from B. Vogelstein (Johns Hopkins Cancer Center, Baltimore, MD) and were maintained as previously described (23). McCoy's 5A medium was supplemented with different concentrations of doxycycline, for example, 0 (D.0), 1 (D.1), 2 (D.2), and 5 ng/mL (D.5). For *in vivo* amino acid–coded tagging (AACT) of the proteome and for proteomic analysis, the DLD-1.vector or DLD-1.PUMA cells were first maintained in the α-MEM medium supplemented with 10% v/v dialyzed fetal bovine serum, and antimicrobial reagents in the presence of 20 ng/mL of doxycycline (D.20). For induction, DLD-1.PUMA cells were cultured in AACT-α-MEM, in which the normal lysine (Lys_{D0}) was completely substituted by Lys_{D4} as described previously (36, 37). Near 60% confluency, the adherent cells were rinsed with PBS and refed with the induction medium (i.e., AACT-α-MEM without doxycycline) for 1 hour to induce PUMA and apoptosis. Human fibroblast cells (American Type Culture Collection, Manassas, VA) were maintained in DMEM medium supplemented with 10% fetal bovine serum, antimicrobial reagents, and 2 mmol/L L-glutamine.

Apoptosis Assay. Cells were plated on P100 plates and grown to 70% to 80% confluency in D.20 medium, rinsed with PBS, and refed with different induction media, D.0, D.1, D.2, and D.5. After incubation for various times, attached cells were harvested and counted using a hemocytometer. To confirm that cell death was due to apoptosis, total cells including floating cells were collected by centrifugation and stained with Hoechst 33258 (23). Multinucleated cells observed under the fluorescence microscope (Olympus, Tokyo, Japan) were considered to be apoptotic cells.

Semiquantitative Reverse Transcription–PCR. To investigate PUMA expression in induced DLD-1.PUMA cells, semiquantitative reverse transcription–PCR (RT-PCR) was conducted. Total RNA was isolated from the indicated cells using Purescript (Gentra System, Minneapolis, MN). RT was conducted using random hexamers as primers and PCR was conducted using PUMA- specific primers and a standard protocol (23). The primers were forward, 5′-TCCTCAGCCCTCGCTCTCGC-3′, and reverse, 5′-CCGATGCTGAGTCCATCAGC-3′.

Antioxidant and H_2O_2 Treatment of Cells, Reactive Oxygen Species Detection, and Measurement by Dihydroethidium Staining and EPR Spectroscopy. DLD-1.PUMA and DLD-1.vector cells were grown in D.20 medium to 60% confluency and diphenyleneiodonium was added 8 hours before induction. The number of attached cells was determined 2 to 6 hours after culturing in indicated media.

To assay ROS generation in induced DLD-1.PUMA cells using the fluorescence dye dihydroethidium (38), cells were plated on a glass slip in P25 plates in D.20 medium with or without 1 μmol/L diphenyleneiodonium. After incubation for 8 hours, cells were transferred to the indicated induction medium with or without 1 μmol/L diphenyleneiodonium. After incubation for 0, 30, and 90 minutes, dihydroethidium was added to the cell culture (final concentration, 2 μmol/L). Cells were then incubated for an additional 30 minutes, washed twice with PBS, and fixed with 10% (v/v) PBS-buffered formaldehyde. Coverslips were mounted on glass slides, observed under a fluorescence microscope, and the images were captured using a digital camera (Olympus). For H_2O_2 treatment, DLD-1. vector cells were grown on cover glasses, treated with 5 mmol/L H_2O_2 for 1, 2 or 4 hours and observed under fluorescence microscope.

For EPR spectroscopy, DLD-1.PUMA and DLD-1.vector cells were cultured in D.0 or D.20 medium for 30, 60, and 120 minutes, harvested and transferred to PBS containing the spin trapping agent, 1-hydroxy-4-phosphono-oxy-2,2,6,6,-tetramethylpiperidine (PP-H) as previously described (39). The EPR spectra of ROS were recorded using an Elexsys EPR spectrometer (Bruker, Wissembourg, France). The EPR settings for all the experiments were as follows: microwave frequency, 9.8 GHz; field sweep, 75 G; microwave power, 0.6 mW; modulation amplitude, 1.0 G; time constant 5 milliseconds; conversion time, 20.5 milliseconds; sweep time, 21 seconds; receiver gain, 60 dB as previously described (40).

Inhibition of Reactive Oxygen Species Generation by BAX-Inhibiting Peptide. A cell-permeable peptide, BAX-inhibiting peptide (H-VPMLK-OH; EMD Biosciences) was used to determine if Bax is associated with the generation of ROS (41). Stock solutions of BAX-inhibiting peptide and negative control peptide (H-IPMIK-OH, EMD Biosciences) were prepared in PBS and directly added into D.20 medium 1 hour before cells were treated with D.1 medium with the same concentration of BAX-inhibiting peptide or negative control peptide. The final concentration of peptide was 200 μmol/L. Two hours later, dihydroethidium staining was carried out as described above.

Quantitative Proteomics. Induced and AACT-labeled DLD-1.PUMA cells were mixed in equal numbers with uninduced and unlabeled DLD-1.PUMA cells and lysed in 1× SDS-PAGE loading buffer. Total cell extracts were subjected to one-dimensional SDS-PAGE, isolation of protein bands, trypsin digestion, and peptide extraction. Proteomic liquid chromatography and QSTAR tandem mass spectroscopy analysis were carried out as previously described (36, 37). We compared the peak areas of unlabeled and labeled peptides. Peptides that showed altered ratios in the paired unlabeled and labeled peaks were subjected to a sequence search (36, 37).

Immunoblotting. Total cellular extracts from attached cells were obtained by dissolving the cells in radioimmunoprecipitation assay buffer solution (1% sodium deoxycholate, 0.1% SDS, 1% Triton X-100, 0.01 mol/L Tris-Cl, 0.14 mol/L NaCl, pH 8.0). Protein concentration was determined using the bicinchoninic acid method (Pierce, Rockford, IL). Proteins were separated on a 10% SDS-PAGE (20 μg protein/lane) and transferred to polyvinylidene difluoride membranes (Millipore, Bedford, MA) which were then incubated with primary antibodies to stathmin (Cell Signaling Technology, Beverly, MA), catalase (Calbiochem, San Diego, CA), SOD1 (Calbiochem), SOD2 (Calbiochem), α-tubulin (Sigma) and β-actin (Oncogene Research Products, La Jolla, CA), respectively. Subsequently, the blots were incubated with respective horseradish peroxidase–labeled secondary antibodies (Bio-Rad, Hercules, CA). α-Tubulin and β-actin were used as loading control. Proteins were detected using enhanced chemiluminescence (ECL+, Amersham) plus Western blotting detection system (Amersham Biosciences, Piscataway, NJ).

Inhibition of Proteasome Degradation. DLD-1.PUMA cells were pretreated in growth medium containing 20 μmol/L of ALLN for 6 hours and then subjected to PUMA induction by feeding the cells with the induction medium containing 20 μmol/L of ALLN as previously described (42).

PUMA Adenovirus Infection. Construction, amplification and assaying for titers of PUMA adenovirus (Ad-PUMA), and viral infection of mammalian cells were done as previously described (26). Human fibroblast cells were infected with control adenovirus or Ad-PUMA with a range of concentrations from 0.01 to 5 multiplicity of infection (or plaque-forming units per cell, which was estimated to be 0.2-100 virus particles per cell) for indicated times. Cell numbers and apoptosis were measured over time by cell counting and Hoechst 33258 nuclear staining (26).

Immunofluorescent Microscopy. DLD-1.PUMA, DLD-1.vector, or fibroblast cells were grown on glass coverslips, treated as indicated, fixed in 4% (v/v) paraformadehyde solution, blocked with 3% (w/v) bovine serum albumin (BSA), and then incubated in 3% BSA containing anti-α-tubulin antibody (1:2000). Subsequently, coverslips were incubated in 3% BSA containing Texas Red–labeled secondary antibody (1:1000, Jackson Immuno Research, West Grove, PA), rinsed with HEPES-buffered saline, mounted (with or without DAPI staining), and subjected to fluorescent microscope analysis.

Statistical Analysis. Data are expressed as mean ± SE. Comparison between experimental groups was made using Student's *t* test. A *P* value of <0.05 was considered statistically significant.

Results

PUMA Induces Dose- and Time-Dependent Apoptosis. Using "Tet-off" inducible DLD-1.PUMA cells, we previously showed that PUMA could induce a rapid, *p53*-independent (because DLD-1 cells are *p53* null), BAX-dependent, and mitochondrial-mediated apoptosis in DLD-1 cells (23, 26). Phenotypes in apoptotic DLD-1.PUMA cells include chromatin condensation, release of cytochrome *c* and activation of caspases 9 and 3 (23, 26). However, the molecular mechanism underlying PUMA-induced apoptosis is not well understood. Because PUMA expression is regulated by the concentration of doxycycline in the medium, we reevaluated PUMA-induced apoptosis in DLD-1 cells in a dose- and time-dependent manner for the determination of the optimal induction conditions for EPR and proteomics analyses (see below). DLD-1.PUMA cells were cultured in medium containing different concentrations of doxycycline for various times and assayed for apoptosis by Hoechst 33258 staining. For dose-dependent analysis, a cell growth curve was obtained using various doxycycline concentrations. As shown in Fig. 1*A*, the number of surviving cells decreased as the doxycycline concentration decreased. When the doxycycline concentration in the medium was <5 ng/mL, a statistically significant decrease in adherent cells was obtained ($P < 0.05$). Expression of PUMA in DLD-1.PUMA cells was examined using semiquantitative RT-PCR. As expected, PUMA expression decreased as the doxycycline concentration increased (Fig. 1*B*). In the time course experiment, a significant decrease in the number of attached cells compared with control was obtained after cells were refed D.0 medium for 6 hours (Fig. 1*C*). Semiquantitative RT-PCR showed a time-dependent increase (>3-fold) in PUMA expression as early as 20 minutes after induction (Fig. 1*D*). Induction of PUMA was even more significantly increased (>8-fold) 60 minutes after, which was consistent with our previous observation of time course induction of PUMA at the protein level (23).

Diphenyleneiodonium, a Reactive Oxygen Species Inhibitor, Partially Blunts PUMA-Induced Apoptosis and Reactive Oxygen Species Generation in DLD-1.PUMA Cells. To determine if PUMA-induced apoptosis was related to increased ROS generation, the effect of diphenyleneiodonium on cell survival was tested. Previously, diphenyleneiodonium, a ROS inhibitor and a potent antioxidant, has been shown to be an inhibitor of *p53*-induced apoptosis (9). Our results showed that diphenyleneiodonium partially protected induced DLD-1.PUMA cells (Fig. 2*A*) and is consistent with the finding that diphenyleneiodonium blocks *p53*-induced ROS generation and apoptosis in DLD-1 cells (9). Because it is an essential downstream effector of *p53*-mediated apoptosis, PUMA may play an important role in the induction of ROS generation. To further evaluate if diphenyleneiodonium-inhibited ROS generation could decrease PUMA-induced apoptosis, we first examined whether diphenyleneiodonium alone resulted in cytotoxicity of DLD-1.PUMA cells. We conducted a preliminary diphenyleneiodonium dose-dependent cytotoxicity experiment and found that >5 μmol/L of diphenyleneiodonium

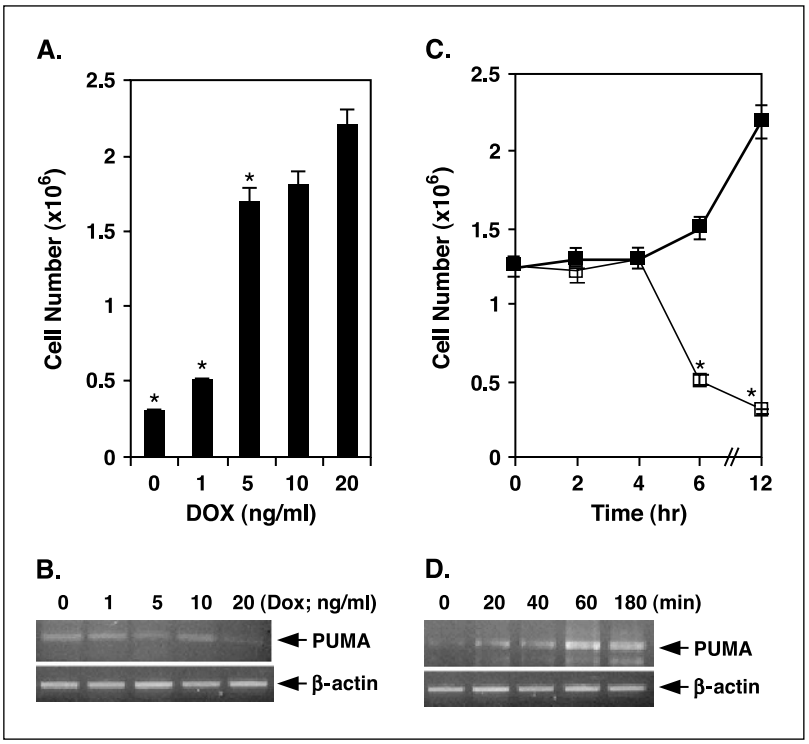

Figure 1. Time- and dose-dependent induction of PUMA and apoptosis in DLD-1.PUMA cells. *A,* PUMA induces dose-dependent apoptosis. DLD-1.PUMA cells were cultured in medium containing doxycycline (DOX; ng/mL) as indicated. Attached cells were harvested and counted after 24 hours. *B,* PUMA expression is regulated by doxycycline concentration. Semiquantitative RT-PCR using total RNA isolated from cells treated with media containing different concentrations of doxycycline as indicated for 30 minutes. *C,* PUMA induces time-dependent apoptosis. DLD-1.PUMA cells were cultured in D.20 (DOX, 20 ng/mL) medium (■) or D.0 (DOX, 0 ng/mL) medium (□), harvested, and counted at the times indicated. *D*, induction of PUMA expression is time dependent. Semiquantitative RT-PCR using total RNA isolated from cells grown in D.0 medium for the indicated time. Each experiment was repeated at least thrice. *, $P < 0.05$, significant difference compared with control by Student's *t* test.

was toxic to DLD-1.PUMA (>50% of cell death; data not shown). Subsequently, a test was conducted to determine the ability of diphenyleneiodonium to protect induced DLD-1.PUMA cells. As shown in Fig. 2*B*, 1 μmol/L diphenyleneiodonium improves cell survival in D.1 and D.2 medium: it did partially protect cells from apoptosis in two induction media (D.1 and D.2) containing diphenyleneiodonium.

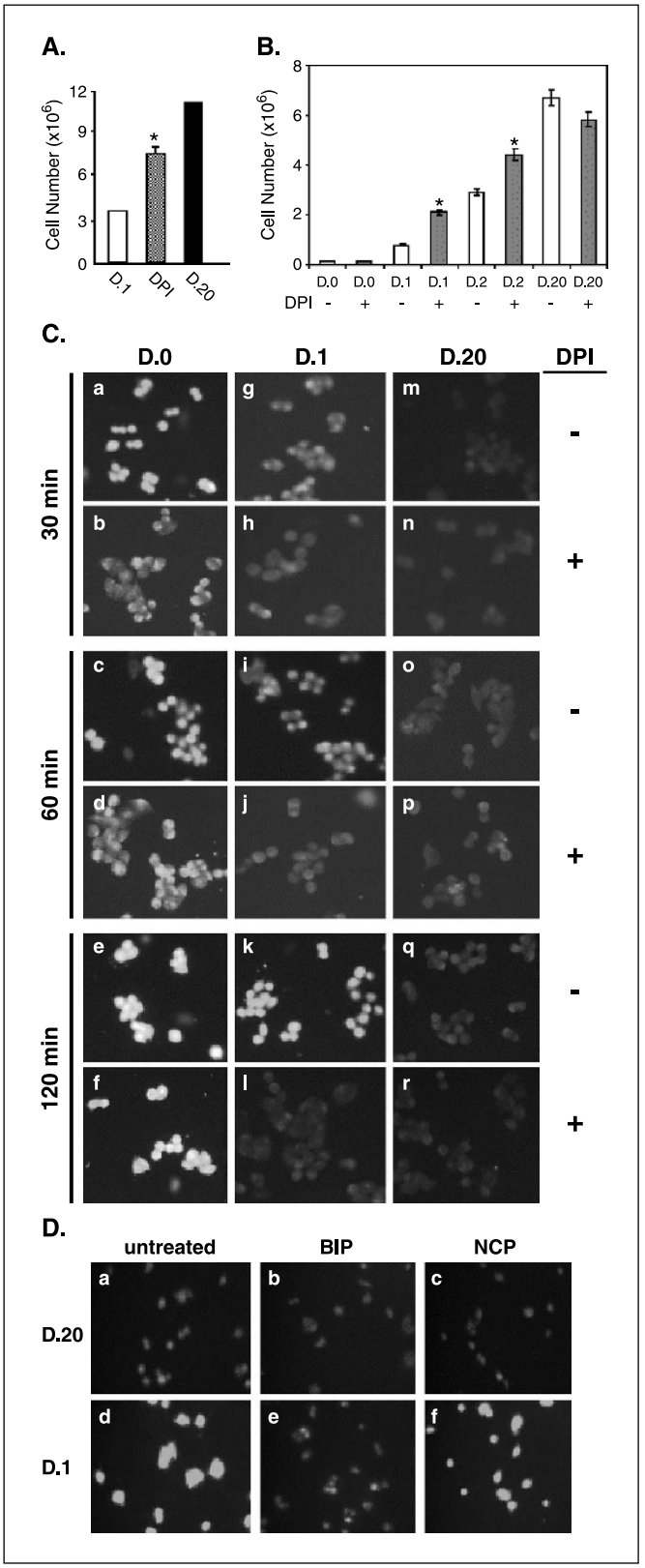

Figure 2. Detection and blocking of ROS in induced DLD-1.PUMA cells. *A,* the effect of diphenyleneiodonium (*DPI*) on apoptosis of DLD-1.PUMA cells. Diphenyleneiodonium significantly decreased apoptosis in induced DLD-1.PUMA cells grown in D.1 (doxycycline, 1 ng/mL). *B,* diphenyleneiodonium blocks apoptosis in induced DLD-1.PUMA cells. Diphenyleneiodonium (1 μmol/L) effectively protected cells from apoptosis in the induction media D.1 + diphenyleneiodonium and D.2 (doxycycline, 2 ng/mL) + diphenyleneiodonium as compared with those of D.1 and D.2, respectively. Each experiment was repeated at least thrice. *, $P < 0.05$, significant difference compared with the respective samples without diphenyleneiodonium by Student's *t* test. *C,* diphenyleneiodonium blunts ROS generation in induced DLD-1.PUMA cells. Concentration of doxycycline and time of PUMA induction (minutes) were as indicated. *D,* BAX-inhibiting peptide (*BIP*) blunts the generation of ROS in induced DLD-1.PUMA cells. Cells with or without peptide treatment were as indicated. *NCP,* negative control peptide. Representative data from four such experiments. All the dihydroethidium staining images of (*C*) and (*D*) were taken by the same microscope (BH2-RFCA, Olympus) with the charge-coupled device camera (Optronics 60806, Olympus) and the same parameters (e.g., exposure time, 7.6 milliseconds).

Detection of Reactive Oxygen Species Generation by Dihydroethidium Staining. We used two methods to directly detect the generation of ROS in PUMA-induced cells, namely dihydroethidium staining and EPR spectroscopy. In dihydroethidium staining, superoxide radicals were detected as early as 30 minutes after the cells were refed D.0 medium (Fig. 2*C*, *D.0*, *a*, *c*, and *e*). This result is consistent with the semiquantitative RT-PCR result that PUMA expression is induced as early as 20 minutes after induction (Fig. 1*D*, *lane 2*). Furthermore, depending on the level of PUMA expression, significantly higher levels of superoxide radicals were detected in cells fed with D.0 (Fig. 2*C*, *a*, *c*, and *e*) than in cells fed with D.1 (Fig. 2*C*, *g*, *i*, and *k*) or D.20 (Fig. 2*C*, *m*, *o*, and *q*). In cells in D.0 or D.1 medium, generation of superoxide radicals was time dependent and was markedly higher after 120 minutes induction than at 30 and 60 minutes (Fig. 2*C*, *e* and *k* versus *a* and *g*; *e* and *k* versus *c* and *i*, respectively). Following quantification of dihydroethidium staining intensity, we showed that diphenyleneiodonium inhibited the generation of superoxide radicals by ~75% in cells in D.1 medium (Fig. 2*C*, *h* versus *g*, *j* versus *i*, and *l* versus *k*).

BAX-Inhibiting Peptide Ablates Reactive Oxygen Species Increase in PUMA-Overexpressing Cells. To investigate if BAX was important to PUMA-induced ROS generation and apoptosis, we utilized a BAX-inhibiting peptide, which sequesters BAX and blocks BAX translocation from the cytosol to mitochondria and prevents the formation of functional BAX complexes (41). BAX-inhibiting peptide also provides cytoprotection against Bax-mediated apoptosis (41). Previously, we showed that PUMA overexpression induced BAX oligomerization in mitochondria and apoptosis in DLD-1 cells (26). In the present study, we cultured DLD-1.PUMA cells in D.20 + dihydroethidium or D.1 + dihydroethidium medium in the presence or absence of BAX-inhibiting peptide and examined the dihydroethidium staining intensity. As shown in Fig. 2*D*, BAX-inhibiting peptide markedly inhibited (>90%) the generation of ROS in induced DLD-1.PUMA cells cultured in D.1 medium (Fig. 2*D*, *e*) when compared with those of the untreated cells or cells treated with negative control peptide (Fig. 2*D*, *d* and *f*). Taken together with the previous findings (26, 41), these data suggest that the ROS generation through PUMA-overexpression is mediated by functional BAX.

Measurement of Reactive Oxygen Species Generation in DLD-1.PUMA Cells by EPR Spectroscopy. EPR in combination with spin trapping is the most specific and definitive method for

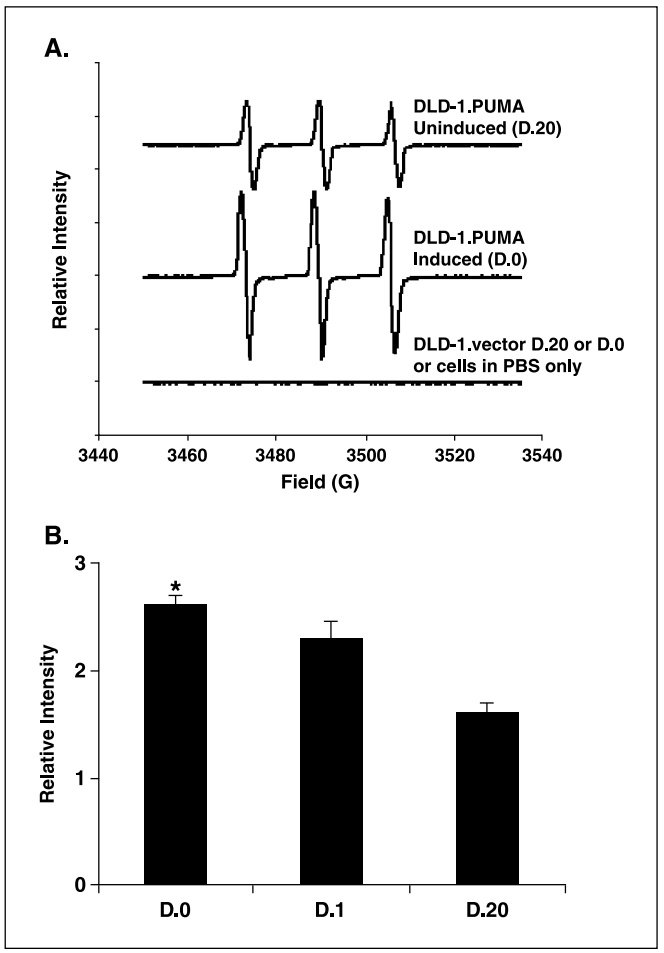

Figure 3. Detection of intracellular ROS in induced DLD-1.PUMA cells using EPR spectroscopy. *A,* EPR spectra and the relative intensity of the PP-H radical intermediates in uninduced (D.20) and induced (D.0) DLD-1.PUMA and DLD-1.vector cells. Cells resuspended in PBS only were also used as controls. *B,* relative amount of ROS generated in DLD-1.PUMA cells in *A*. *, $P < 0.05$, significant difference comparing to the respective samples of D.20 by Student's *t* test.

the detection of free radicals (43). The spin-trapping agent PP-H has been shown to react with superoxide radicals to produce stable intermediates (39). Superoxide radicals trapped by PP-H display a standard three-peak pattern that can be observed in the range of 3460 to 3520 G (Fig. 3*A*; ref. 39). EPR spectroscopy revealed that there were no ROS signals that could be detected in induced or uninduced DLD-1.vector cells or cells resuspended in PBS in the absence of PP-H (Fig. 3*A*). In contrast, there was a significant increase of superoxide radicals (>1.6-fold) in DLD-1.PUMA cells fed with D.0 medium for 2 hours compared with control cells fed with D.20 medium (Fig. 3*A* and *B*). ROS signals could be detected in induced DLD-1.PUMA cells as early as 30 minutes after induction (data not shown). The ROS signals that were detected in uninduced DLD-1.PUMA cells might be due to the leaky expression of PUMA.

Early Regulated Proteins in PUMA-Induced Apoptosis in DLD-1.PUMA Cells. Mitochondria-mediated apoptosis involves a variety of protein alterations (3, 4, 6). To identify regulated proteins that might be influenced by early ROS generation and play important roles in this system, quantitative proteomic profiling of differentially regulated proteins of PUMA-induced versus uninduced DLD-1.PUMA cells was conducted. The results showed several proteins that were unchanged, up-regulated, or down-regulated 1 hour after PUMA-induced oxidative stress. As shown in Table 1 (see also Supplemental Fig. S1), cyclophilin A, chaperonin 10, α-tubulin, β-tubulin, and Cu/Zn superoxide dismutase 1 (SOD1) were unchanged; the expression of the oxidative stress–responded protein peroxiredoxin 1 was increased (>1.34×). We also found that heat shock protein 70 (>1.48×) and pyruvate kinase M2 (>1.39×) were up-regulated. In the same experiment, we also found that stathmin and polyadenylic acid binding protein 1 were down-regulated (by 25% and 22%, respectively) in induced DLD-1.PUMA cells. To confirm and extend the observations of the proteomic analysis, we conducted immunoblotting assays and showed that there was no change in SOD1, SOD2, and catalase. In contrast, a decreased expression of stathmin was found as early as 40 minutes in cells cultured in D.0 medium (Fig. 4*A*). To further investigate if PUMA-induced stathmin down-regulation was a general phenomenon, we turned to human fibroblast cells, a well-established model for studying stathmin and microtubule regulation (32). We infected human fibroblasts with Ad-PUMA for 12 hours and showed that stathmin was down-regulated in PUMA-overexpressing fibroblasts (Fig. 4*B*).

Down-regulation of Stathmin Is Mediated through Proteasome Degradation. In previous studies, stathmin has been shown to be down-regulated by *p53* (34, 35). Therefore, to investigate the molecular mechanism responsible for PUMA-induced stathmin down-regulation in DLD-1 cells, we reasoned that stathmin may be subjected to proteasome-mediated degradation in apoptotic pathway. We treated DLD-1.PUMA cells with a well-established proteasome inhibitor, ALLN (42). We found that the levels of stathmin remained unchanged over a 2-hour time course in induced DLD-1.PUMA cells in the presence of 20 mmol/L ALLN (Fig. 4*C*). These data suggest that stathmin down-regulation by PUMA overexpression is mediated through proteasome degradation.

Table 1. A short list of unchanged and regulated proteins in response to early PUMA-induced oxidative stress revealed by quantitative proteomic profiling

Protein name	Gene identification no.	Lys_{D4}:Lys_{D0}*
Unchanged		
Superoxide dismutase 1	36535	0.97
Chaperonin 10	4008131	1.01
α-Tubulin	32015	1.02
β-Tubulin	223429	1.04
Cyclophilin A	1431788	1.08
Up-regulated		
Peroxiredoxin 1	4505591	1.34
Heat shock protein 70	21040386	1.48
Pyruvate kinase M2	125604	1.39
Down-regulated		
Stathmin	5031851	0.74
Poly(A) binding protein 1	3183544	0.78

*Lys_{D4}:Lys_{D0}, ratio of Lys_{D4}-labeled peptide and Lys_{D0}-labeled counterpart.

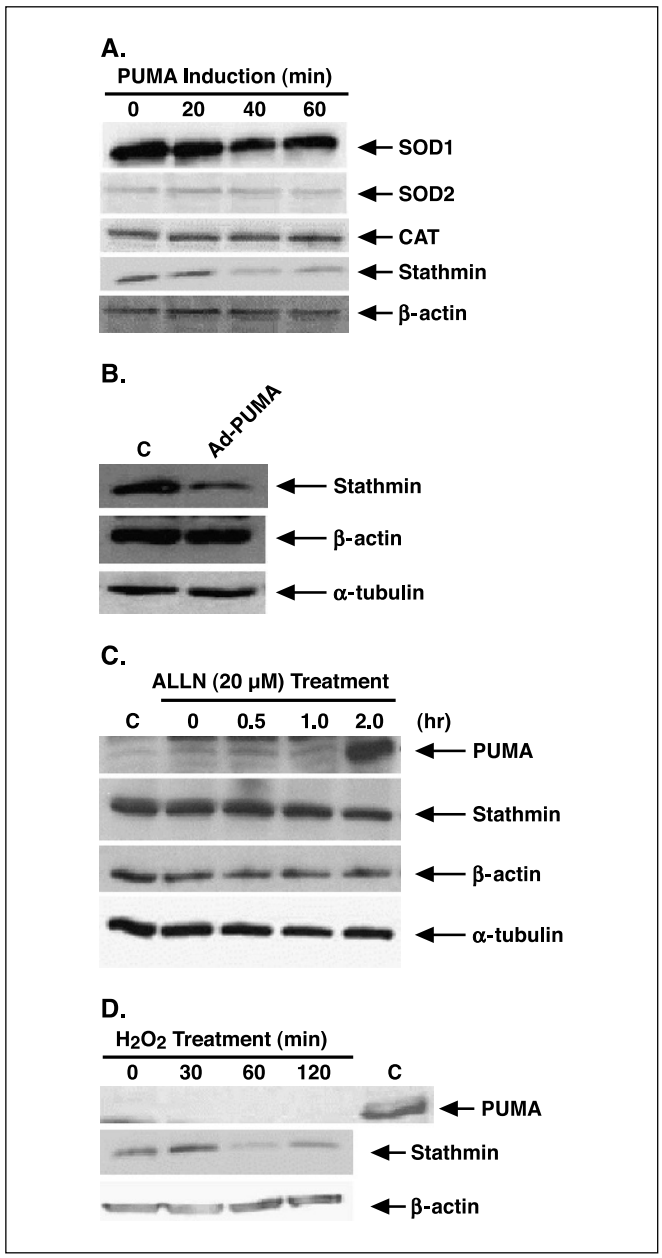

Figure 4. Immunoblotting analysis. *A,* time course of expression of SOD1, SOD2, stathmin, and catalase (*CAT*) in induced DLD-1.PUMA cells. *B,* down-regulation of stathmin in human fibroblast cells infected with PUMA adenovirus (Ad-PUMA). Total soluble proteins were isolated from fibroblasts 12 hours after infection with control adenovirus or Ad-PUMA. *C,* down-regulation of stathmin by PUMA overexpression is mediated through proteasome degradation. DLD-1.PUMA cells were pretreated with 20 mmol/L ALLN 6 hours before the induction of PUMA expression. Total soluble proteins were isolated from induced cells in time course (hours). *D,* time course expression of PUMA and stathmin in H_2O_2-treated DLD-1.vector cells. β-Actin and α-tubulin were used as loading control.

Down-regulation of Stathmin in H_2O_2-Treated Cells. Our proteomic profiling and immunoblotting analysis found that stathmin was one of the proteins down-regulated early (1 hour after induction of PUMA expression) in induced DLD-1.PUMA cells. To investigate if the down-regulation of stathmin was associated with high intracellular H_2O_2, time-dependent expression of stathmin was determined using immunoblotting analysis in H_2O_2-treated DLD-1.vector cells. As shown in Fig. 4*D*, a decrease (by 75%) in stathmin was confirmed in DLD-1.vector cells treated with 5 mmol/L H_2O_2 for 1 hour (Fig. 4*D*). In contrast, PUMA protein could not be detected in DLD-1.vector cells treated with 5 mmol/L H_2O_2 over a course of 2 hours (Fig. 4*D*), indicating that the level of endogenous PUMA is low in DLD-1 cells and there was no significant induction of PUMA in early H_2O_2 treatment. In summary, these results indicate that expression of stathmin can be down-regulated by H_2O_2 and does not require the presence of PUMA protein.

PUMA-Induced Reactive Oxygen Species Generation Promotes Disorganization of Cytoplasmic Microtubule Network in Apoptosis. We showed that PUMA overexpression induced both ROS generation and stathmin degradation. Stathmin and other microtubule regulatory proteins play important roles in regulating mitotic spindles (32). Taken together, we reasoned that ROS and stathmin, and possibly other regulated proteins, may play roles in regulating cellular microtubule network in apoptosis. The relationship between stathmin status (e.g., phosphorylation, stability, and degradation) and microtubule network in apoptosis has not been explored previously. Therefore, we examined the organization of the cellular microtubule network by immunostaining using an antibody to α-tubulin. DLD-1 cells have large nuclei that occupy approximately two thirds of the cell volume. As shown in Fig. 5*A*, normal microtubules exhibited cytosolic, threadlike structures. In contrast, after treating cells with either PUMA overexpression or H_2O_2 for 2 to 4 hours, microtubules displayed depolymerized and dispersed structures throughout the cytoplasm (Fig. 5*A*, *c*, *d*, *g*, and *h*). These data suggest that ROS induce disorganization/disruption of the cellular microtubule network. We also investigated the effect of PUMA overexpression on microtubule network in human fibroblasts. We infected fibroblasts with Ad-PUMA and showed that PUMA overexpression also induced disorganization/disruption of cellular microtubule network in apoptotic fibroblasts (Fig. 5*B*, *d* and *e* versus *a* and *b*).

Discussion

To investigate if PUMA overexpression induced ROS generation, we used two different physical-chemical methods. The first, dihydroethidium staining, is a widely used method to detect the presence of ROS in cells. Using this method, we showed that overexpression of PUMA induced ROS generation. The second approach (EPR spectroscopy) confirmed this conclusion. EPR techniques are more specific and definitive than fluorescence dye assays in the detection of ROS, especially when they are used in conjunction with spin-trapping agents. EPR spectroscopy is quantitative (39, 40, 43). To select a specific spin-trapping agent, there are many nitrone and nitroso compounds to choose from, depending on the nature of the specific reactive species. In our present study, we used a new, cyclic hydroxylamine, PP-H, which has been shown to react with superoxide radicals to produce the stable adducts. PP-H has superior sensitivity over 5-diethoxyphosphoryl-5-methyl-1-pyrroline-*N*-oxide (DEPMPO) for superoxide detection and can measure a 10-fold lower superoxide radical formation rate than DEPMPO (39). Using PP-H in EPR spectroscopy, we found that our EPR methodology was sufficiently sensitive to detect intracellular ROS signals and confirm ROS generation in DLD-1.PUMA cells. PUMA-overexpressing and apoptotic cells showed a significantly higher ROS signal (>1.67-fold) compared with that of normal

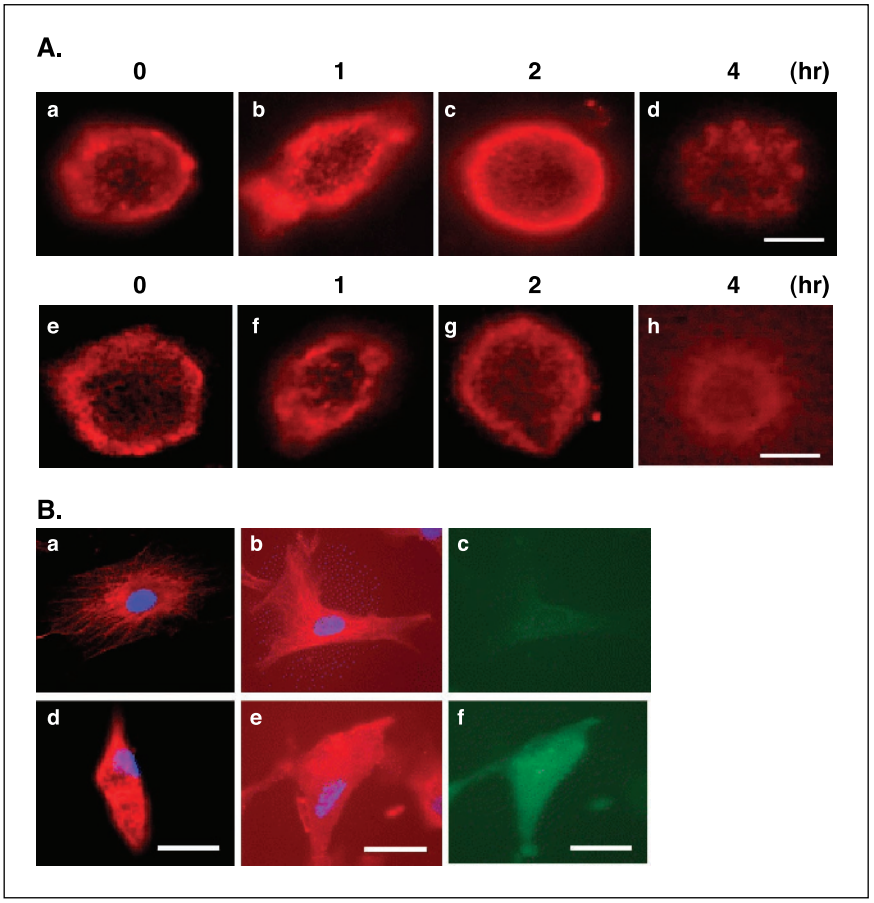

Figure 5. PUMA overexpression and H_2O_2 treatment promote disorganization of the microtubule network in cells. Time course of immunofluorescent staining of α-tubulin (*red*) in (*A*) induced DLD-1.PUMA cells (*a–d*) and DLD-1.vector cells treated with 5 mmol/L H_2O_2 *(e–h)* and (*B*) human fibroblasts infected with control adenovirus or Ad-PUMA for 12 hours. *a* and *b,* cells infected with control adenovirus in two independent experiments. *d* and *e,* cells infected with Ad-PUMA in two independent experiments. *c* and *f,* are the green fluorescent protein images of *b* and *e*, respectively. *a*, *b*, *d*, and *e*, Hoechst 33258 nuclear staining (*blue*). PUMA overexpression in the Ad-PUMA–infected fibroblasts was shown by the elevated green fluorescent protein expression (*f*). At least 300 cells were analyzed for each experiment. *Bars*, 10 μm.

DLD-1.PUMA cells. As far as we know, this is the first verification by EPR analysis that overexpression of a proapoptotic gene induces ROS generation.

Three lines of evidence suggest that the predominant ROS generated by PUMA overexpression are superoxide radicals and H_2O_2. First, dihydroethidium has been proposed to preferentially interact with superoxide radicals (38). Second, the spin-trapping agent PP-H used in our EPR analysis is sensitive in detecting superoxide radical. The EPR spectra showed a classic three-peak pattern of PP-H reacting with superoxide radical (Fig. 3*A*). Third, proteomic profiling showed that peroxiredoxin 1 and heat shock protein 70 were up-regulated by PUMA-induced ROS generation and oxidative stress (Table 1; Supplemental Fig. S1). Previously, peroxiredoxin 1 has been shown to be induced by H_2O_2 treatment in cancer cells (44) and human endothelial cells (45). Therefore, we suggest that down-regulation of stathmin in apoptotic DLD-1.PUMA cells is related to superoxide and H_2O_2 overproduction.

A wealth of literature has documented that the dynamics of microtubule polymerization and depolymerization during the cell cycle are regulated by stathmin. When unphosphorylated, stathmin promotes microtubule depolymerization during interphase and late mitosis (29–32, 46). In addition, Johnsen and colleagues (35) reported that down-regulation of stathmin expression is associated with G_2-M cell cycle arrest and that constitutive overexpression of stathmin overcomes *p53*-mediated G_2-M cell arrest. However, the role of stathmin and microtubules in apoptosis has not been previously explored. In the present study, we found that PUMA overexpression and ROS generation induced stathmin degradation and disruption of the cellular microtubule network in apoptotic cells. Regarding the time course, we showed that the induction of PUMA in DLD-1.PUMA cells could be identified as early as 20 to 30 minutes (Fig. 1*D* and 4*C*) after induction followed by ROS generation at ~30 minutes (Fig. 2*C*, *a* and *g*), stathmin degradation at ~40 minutes, and disruption of cellular microtubule network at ~2 to 4 hours (Fig. 5*A*, *c* and *d*). We also showed stathmin degradation could be induced by H_2O_2 treatment in DLD-1 cells independent of *p53* and PUMA (Fig. 4*D*). Based on the results, we suggest that PUMA induces apoptosis, in part by generating ROS and altering protein expression, such as proteasome-mediated stathmin degradation. Down-regulation of stathmin, together with other regulated proteins, directly or indirectly regulate the cell microtubule network in apoptotic cells.

Mitochondrial translocation and multimerization of Bax is a critical event in mitochondrial-mediated apoptosis. PUMA, a mitochondrial membrane protein, induces apoptosis by translocating functional BAX complexes onto the mitochondrial outer membrane (26, 47). We found that BAX-inhibiting peptide not only blocks formation of functional BAX on the mitochondrial membrane but also greatly (>90%) inhibited the generation of ROS in PUMA-overexpressing cells. It has been shown that ROS formation during neuronal cell death occurs downstream from Bax translocation (21, 48, 49). There are several questions that deserve further investigation. First, PUMA seems to induce ROS generation through functional BAX on the mitochondrial membrane and BAX has been shown to function as a pore to "release" cytochrome *c* from mitochondria (3, 6, 50), this raises the question as to how functional

BAX induces ROS generation and whether mitochondrial BAX may function as a pore/transporter to release ROS? Second, does stathmin serve as a ROS sensor in the cytosol that "transports" ROS-initiated signals to other organelles, such as nucleus? A better understanding of the molecular bases of ROS-induced apoptosis will not only benefit cancer therapeutics but also other diseases such as atherosclerosis, neurologic diseases, and AIDS. Finally, DLD-1.PUMA cells provide an excellent model for genomics and proteomics investigation of oxidative stress–induced apoptosis.

Acknowledgments

Received 5/18/2004; revised 12/28/2004; accepted 12/29/2004.

Grant support: Howard Hughes Medical Institute Research grant-in-aid to the UNM Cancer Research Facility, American Cancer Society institutional research grant (ACS-IRG 412488-00095), and UNM-Research Allocation grant (C-2222-RAC).

The costs of publication of this article were defrayed in part by the payment of page charges. This article must therefore be hereby marked advertisement in accordance with 18 U.S.C. Section 1734 solely to indicate this fact.

We thank Dr. Bert Vogelstein for kindly providing us the cell lines, DLD-1.PUMA and DLD-1.vector and Drs. James M. Phang and Laurel Sillerud for reading this manuscript.

References

1. Igney FH, Krammer PH. Death and anti-death: tumour resistance to apoptosis. Nat Rev 2002;2:277–88.
2. Joza N, Susin SA, Daugas E, et al. Essential role of the mitochondrial apoptosis-inducing factor in programmed cell death. Nature 2001;410:549–54.
3. Wang X. The expanding role of mitochondria in apoptosis. Genes Dev 2001;15:2922–33.
4. Zamzami N, Kroemer G. The mitochondria in apoptosis: how Pandora's box open. Nat Rev Immunol 1999;17:781–828.
5. Green DR. Apoptotic pathways: the roads to ruin. Cell 2002;94:695–8.
6. Scorrano L, Korsmeyer SJ. Mechanisms of cytochrome *c* release by proapoptotic BCL-2 family members. Biochem Biophys Res Commun 2003;304:437–44.
7. Vogelstein B, Lane D, Levine AJ. Surfing the p53 network. Nature 2000;408:307–10.
8. Vousden KH, Lu X. Live or let die: the cell's response to p53. Nat Rev Cancer 2002;2:594–604.
9. Polyak K, Xia Y, Zweier JL, Kinzler KW, Vogelstein B. A model for p53-induced apoptosis. Nature 1997;389:300–5.
10. Johnson TM, Yu ZX, Ferrans VJ, Lowenstein RA, Finkel T. Reactive oxygen species are downstream mediators of p53-dependent apoptosis. Proc Natl Acad Sci U S A 1996;93:1848–52.
11. Macip SM, Igarashi M, Berggren T, Yu J, Lee SW, Aaronson SA. Influence of induced reactive oxygen species in p53-mediated cell fate decisions. Mol Cell Biol 2003;23:8576–85.
12. Donald SP, Sun XY, Hu C-AA, et al. Proline oxidase, encoded by p53-induced gene-6, catalyzes the generation of proline-dependent reactive oxygen species. Cancer Res 2001;61:1810–5.
13. Maxwell SA, Rivera A. Proline oxidase induces apoptosis in tumor cells, and its expression is frequently absent or reduced in renal carcinomas. J Biol Chem 2003;278:9784–9.
14. Raha S, Robinson RH. Mitochondria, oxygen free radicals, and apoptosis. Am J Med Gen 2001;106:62–70.
15. Allen RG, Tresini M. Oxidative stress and gene regulation. Free Radic Biol Med 2000;28:463–99.
16. Martindale JL, Holbrook NJ. Cellular response to oxidative stress: signaling for suicide and survival. J Cell Physiol 2002;192:1–15.
17. Miyashita T, Krajewski S, Krajewska M, et al. Tumor suppressor p53 is a regulator of bcl-2 and bax gene expression *in vitro* and *in vivo*. Oncogene 1994; 9:1799–805.
18. Miyashita T, Reed JC. Tumor suppressor p53 is an activator of the human bax gene. Cell 1995;80:293–9.
19. Oda E, Ohki R, Murasawa H, et al. Noxa, a BH3-only member of the family and candidate mediator of p53-induced apoptosis. Science 2000;288:1053–8.
20. Adams JM, Cory S. The protein family: arbiters of cell survival. Science 1998;281:1322–6.
21. Kirkland RA, Franklin JL. Bax, reactive oxygen, and cytochrome *c* release in neuronal apoptosis. Antioxid Redox Signal 2003;5:589–96.
22. Kirkland RA, Windelborn JA, Kasprzak JM, Franklin JL. A Bax-induced pro-oxidant state is critical for cytochrome *c* release during programmed neuronal death. J Neurosci 2002;22:6480–90.
23. Yu J, Zhang L, Hwang PM, Kinzler KW, Vogelstein B. PUMA induces the rapid apoptosis of colorectal cancer cells. Mol Cell 2001;7:673–82.
24. Nakano K, Vousden KH. PUMA, a novel proapoptotic gene, is induced by p53. Mol Cell 2001;7:683–94.
25. Han J, Flemington C, Houghton AB, et al. Expression of bbc3, a pro-apoptotic BH3-only gene, is regulated by diverse cell death and survival signals. Proc Natl Acad Sci U S A 2001;98:11318–23.
26. Yu J, Wang Z, Kinzler KW, Vogelstein B, Zhang L. PUMA mediates the apoptotic response to p53 in colorectal cancer cells. Proc Natl Acad Sci U S A 2003; 100:1931–6.
27. Villunger A, Michalak EM, Coultas L, et al. p53- and drug-induced apoptotic responses mediated by BH3-only proteins puma and noxa. Science 2003;302:1036–8.
28. Jeffers JR, Parganas E, Lee Y, et al. Puma is an essential mediator of p53-dependent and–independent apoptotic pathways. Cancer Cell 2003;4:321–8.
29. Iancu C, Mistry SJ, Arkin S, Atweh GF. Taxol and anti-stathmin therapy: a synergistic combination that targets the mitotic spindle. Cancer Res 2000;60:3537–41.
30. Abal M, Andreu JM, Barasoain I. Taxanes: microtubule and centrosome targets, and cell cycle dependent mechanisms of action. Curr Cancer Drug Targets 2003; 3:193–203.
31. Belmont LD, Mitchison TJ. Identification of a protein that interacts with tubulin dimers and increases the catastrophe rate of microtubules. Cell 1996;84:623–31.
32. Mistry SJ, Atweh GF. Role of stathmin in the regulation of the mitotic spindle: potential applications in cancer therapy. Mt Sinai J Med 2002;69:299–304.
33. Brattsand G, Roos G, Marklund U, et al. Quantitative analysis of the expression and regulation of an activation-regulated phosphoprotein (oncoprotein 18) in normal and neoplastic cells. Leukemia 1993;7: 569–79.
34. Ahn J, Murphy M, Kratowicz S, Wang A, Levine AJ, George DL. Down-regulation of the stathmin/Op18 and FKBP25 genes following p53 induction. Oncogene 1999;18:5954–8.
35. Johnsen JI, Aurelio ON, Kwaja Z, et al. P53-mediated negative regulation of stathmin/Op18 expression is associated with G(2)/M cell-cycle arrest. Int J Cancer 2000;88:685–91.
36. Pan S, Gu S, Bradbury EM, Chen X. Single peptide-based protein identification in human proteome through MALDI-TOF MS Coupled with amino acids coded mass-tagging. Anal Chem 2003;75:1316–24.
37. Liu Z, Gu S, Pan S, et al. Global investigation of p53-induced apoptosis through quantitative proteomic profiling using comparative amino acid-coded tagging. Mol Cell Proteomics 2004;3:998–1008.
38. Zhao H, Kalivendi S, Zhang H, et al. Superoxide reacts with hydroethidine but forms a fluorescent product that is distinctly different from ethidium: potential implications in intracellular fluorescence detection of superoxide. Free Radic Biol Med 2003; 34:1359–68.
39. Dikalov SI, Dikalova AE, Mason RP. Noninvasive diagnostic tool for inflammation-induced oxidative stress using electron spin resonance spectroscopy and an extracellular cyclic hydroxylamine. Arch Biochem Biophys 2002;402:218–26.
40. Liu KJ, Husler J, Ye J, et al. On the mechanism of Cr(VI)-induced carcinogenesis: dose dependence of cellular responses. Mol Cell Biochem 2001;222:221–9.
41. Sawada M, Hayes P, Matsuyama S. Cytoprotective membrane-permeable peptides designed from the Bax-binding domain of Ku70. Nat Cell Biol 2003;5:352–7.
42. Yu J, Tiwari S, Steiner P, Zhang L. Differential apoptotic response to the proteasome inhibitor bortezomib (VELCADE, PS-341) in Bax-deficient and P21-deficient colon cancer cell. Cancer Biol Ther 2003; 2:694–9.
43. Zweier JL, Kuppusamy P. Electron paramagnetic resonance measurement of free radicals in the intact beating heart: a technique for detection and characterization of free radicals in whole biological tissues. Proc Natl Acad Sci U S A 1988;85:5703–7.
44. Mitsumoto A, Nakagawa Y, Takeuchi A, Okawa K, Iwamatsu A, Takanezawa Y. Oxidized forms of peroxiredoxins and DJ-1 on two-dimensional gels increased in response to sublethal levels of paraquat. Free Radic Res 2001;35:301–10.
45. Mitsumoto A, Takanezawa Y, Okawa K, Iwamatsu A, Nakagawa Y. Variants of peroxiredoxins expression in response to hydrogen peroxide stress. Free Radic Biol Med 2001;30:625–35.
46. Desai A, Mitchison TJ. Microtubule polymerization dynamics. Annu Rev Cell Dev Biol 1997;13:83–117.
47. Liu FT, Newland AC, Jia L. Bax conformational change is a crucial step for PUMA-mediated apoptosis in human leukemia. Biochem Biophys Res Commun 2003;310:956–62.
48. Lee M, Hyun DH, Marshall KA, et al. Effect of overexpression of BCL-2 on cellular oxidative damage, nitric oxide production, antioxidant defenses, and the Proteasome. Free Radic Biol Med 2001;31: 1550–9.
49. Putcha GV, Deshmukh M, Johnson EM Jr. BAX translocation is a critical event in neuronal apoptosis: regulation by neuroprotectants, BCL-2 and caspases. J Neurosci 1999;19:7476–85.
50. Tsujimoto Y. Cell death regulation by the protein family in the mitochondria. J Cell Physiol 2003; 195:158–67.

PUMA Overexpression Induces Reactive Oxygen Species Generation and Proteasome-Mediated Stathmin Degradation in Colorectal Cancer Cells

Zhihe Liu, Huimei Lu, Honglian Shi, et al.

Cancer Res 2005;65:1647-1654.